Optics Communications 474 (2020) 126154

Contents lists available at ScienceDirect

Optics Communications

journal homepage: www.elsevier.com/locate/optcom

Instantaneous non-diffracting light-sheet generation by controlling spatial coherence

Jialei Tang *, Kyu Young Han *

CREOL, The College of Optics and Photonics, University of Central Florida, Orlando, FL, USA

ARTICLE INFO

Keywords:
Non-diffracting beams
Light-sheet
Spatial coherence
LED
Laser

ABSTRACT

We demonstrate single-shot non-diffracting light-sheet generation by controlling the spatial coherence of light. A one-dimensional coherent beam, created by either increasing the spatial coherence of an LED or decreasing the spatial coherence of a laser, makes it unnecessary to scan non-diffracting beams to generate light-sheets. We theoretically and experimentally demonstrate the equivalence between our method and a scanned light-sheet, and investigate the characteristics of the light-sheet in detail. Our method is easily implementable and universally applicable for high-resolution multicolor light-sheet fluorescence imaging.

1. Introduction

Light-sheet illumination was used to investigate the physical properties of colloidal particles a century ago [1]. Since then, concepts from the technique such as orthogonal excitation and detection have found many applications [2]. Over the last two decades light-sheet illumination has been repurposed in light-sheet fluorescence microscopy (LSFM) for biomedical research, and has enabled fast and long-term volumetric imaging of biological specimens with a minimal light level [3–7].

A light-sheet is typically created by a cylindrical lens [3] or by scanning a focused Gaussian beam [8]. Since the imaging field-of-view is set by the Rayleigh range of the propagating Gaussian beam it is strongly coupled with the beam thickness. Thus, LSFM with a larger imaging area unavoidably accompanies a thicker illumination beam, yielding a poor signal-to-background ratio. To solve this problem, a light-sheet, generated by scanning a non-diffracting beam such as a Bessel beam [9,10] or Airy beam [11], has been suggested. This has proven especially useful for high-resolution subcellular imaging due to its capability of providing a thin light-sheet for optical sectioning while maintaining a large field-of-view [10,12]. However, the high peak excitation intensity of a scanning-based light-sheet is likely to increase irreversible photodamage and thus compromises LSFM's superiority for noninvasive imaging of living samples [13,14].

Recently, two intriguing methods have been reported to produce non-diffracting light-sheets. The first is field synthesis [15] where a focused and monochromatic laser line is scanned across an annular mask placed at the objective's pupil plane. Light-sheets with different intensity profiles are generated at each scanning position, and the resulting time-averaged light-sheet is identical to a scanned Bessel beam. The second is a space–time light-sheet [16] where a diffraction grating and phase modulation system such as spatial light modulator (SLM) creates a tight correlation between the spatial and temporal frequencies in broadband incoherent light [17], and this generates universal propagation-invariant light-sheets. Compared to a scanned light sheet [10], field synthesis and space–time light-sheets both provide lower peak excitation intensities, which significantly reduces photodamage in biological specimens [15]. While their working principles are different, both approaches require high spatial coherence of light. Here, we show that controlling the spatial coherence of a light emitting diode (LED) or laser facilitates the generation of static non-diffracting light-sheets without a beam scanning module and/or SLM. We investigate the characteristics of our approach and discuss its implications on LSFM.

2. Single-shot non-diffracting light-sheet generation

Inspired by field synthesis [15], we reason that if numerous focused lines that are spatially incoherent from each other are simultaneously illuminated at the back focal plane (BFP) of objective, one can obtain the same light-sheet profile as the field synthesis [Fig. 1]. Their intensities are simply added up together at the image plane (IP) and this makes it unnecessary to scan and time-average the beam for the light-sheet generation. We note that to realize this idea, a one-dimensional (1D) coherent beam is required, i.e. incoherent along the x-axis but coherent along the y-axis at the conjugated image plane [Fig. 1].

Mathematically, it is straightforward to prove the equivalence between the resulting light-sheets generated by field-synthesis and our approach as follows. We assume that the coherence function of the 1D coherent beam for any two positions (x'_1, y'_1) and (x'_2, y'_2) at the BFP is:

$$G_0\left(x'_1, y'_1; x'_2, y'_2\right) = I(x'_1)\delta(x'_1 - x'_2), \tag{1}$$

* Corresponding authors.
E-mail addresses: jialei.tang@knights.ucf.edu (J. Tang), kyhan@creol.ucf.edu (K.Y. Han).

https://doi.org/10.1016/j.optcom.2020.126154
Received 27 April 2020; Received in revised form 26 May 2020; Accepted 28 May 2020
Available online 30 May 2020

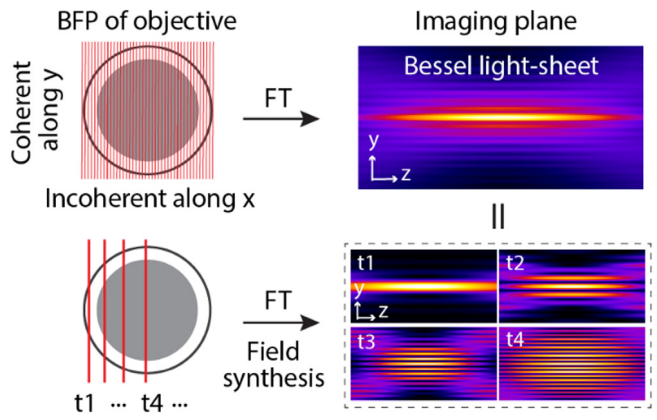

Fig. 1. Working principles of non-diffracting light-sheet generation by single-shot 1D coherent beam (top) compared with field synthesis that sequentially scans a focused line at different time points such as t1 or t4 and averages them (bottom). BFP and FT denote the back focal plane and Fourier transform, respectively.

where $I(x_1')$ is the intensity. Here we have two assumptions: (1) the light source in the y' dimension is completely coherent and the coherence function is equal to 1 for any two positions (y_1' and y_2'); (2) the illumination intensity at BFP is uniform and $I\left(x_1'\right)$ could be regarded as a constant I_0. After transmitting through the optical mask $M(x', y')$ placed at the BFP, the coherence function could be written as [18]:

$$G_{BFP}\left(x_1', y_1'; x_2', y_2'\right) = M^*\left(x_1', y_1'\right) M\left(x_2', y_2'\right) I_0 \delta\left(x_1' - x_2'\right), \tag{2}$$

The amplitude point spread functions from two points $\left(x_1', y_1'\right), \left(x_2', y_2'\right)$ at the BFP to any two points (x_1, y_1), (x_2, y_2) at the IP are represented as $h\left(x_1, x_1'; y_1, y_1'\right)$ and $h\left(x_2, x_2'; y_2, y_2'\right)$, respectively, and they are expressed as $h\left(x, x'; y, y'\right) = h_0 \cdot \exp\left(-ik\frac{(xx'+yy')}{f}\right)$ where h_0 is a constant, k is the wave vector and f is the focal length of the objective lens. Then the coherence function propagating from the BFP to the IP can be described as [18]:

$$\begin{aligned} G_{IP}\left(x_1, y_1; x_2, y_2\right) &= \iint dx_1' dx_2' dy_1' dy_2' G_{BFP}\left(x_1', y_1'; x_2', y_2'\right) \\ &\quad \times h^*\left(x_1, x_1'; y_1, y_1'\right) h\left(x_2, x_2'; y_2, y_2'\right) \\ &= I_0 \iint dx_1' dx_2' dy_1' dy_2' M^*\left(x_1', y_1'\right) M\left(x_2', y_2'\right) \\ &\quad \times \delta\left(x_1' - x_2'\right) h^*\left(x_1, x_1'; y_1, y_1'\right) h\left(x_2, x_2'; y_2, y_2'\right) \\ &= I_0 \int dx_1' \left[\int dy_1' M^*\left(x_1', y_1'\right) h^*\left(x_1, x_1'; y_1, y_1'\right)\right] \\ &\quad \times \left[\int dy_2' \left[M\left(x_2', y_2'\right) h\left(x_2, x_2'; y_2, y_2'\right)\right]\right] \end{aligned} \tag{3}$$

Since $\int dy_1' M(x_1', y_1') h\left(x_1, x_1'; y_1, y_1'\right)$ is equal to a Fourier transform of the mask's transmittance at y' dimension at a fixed position x_1', we represented it as $\mathcal{F}_{y'}(M(x_1', y_1'))$. The intensity distribution at the IP is then calculated as:

$$\langle I(x_1, y_1)\rangle = G_{IP}\left(x_1, y_1; x_1, y_1\right) = I_0 \int dx_1' \left|\mathcal{F}_{y'}(M(x_1', y_1'))\right|^2 \tag{4}$$

where the right side in Eq. (4) represents a (coherent) focused line scanned across the BFP. It is worth noting that $M(x', y')$ can be any mask with optical amplitude and/or phase modulation.

3. Experimental results

We demonstrated our concept experimentally as shown in Fig. 2. First, incoherent light from an LED (λ = 625 nm, M625L4) was collected and collimated by a condenser F1 (f_1 = 20 mm, ACL2520U-A), and focused by a cylindrical lens CL (f_{CL} = 25 mm, LJ4426). The beam passed through a narrow slit S (D = 10 μm, GS-10-N-CG;

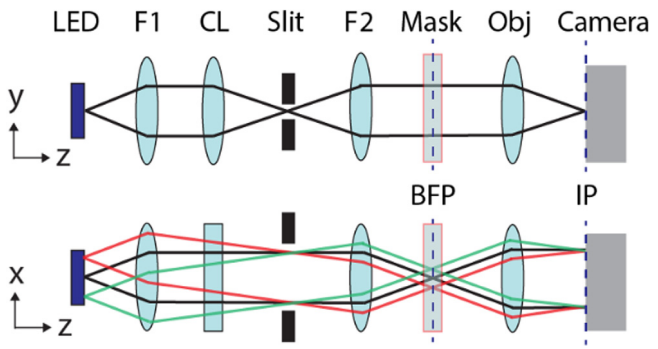

Fig. 2. Experimental scheme of single-shot static light-sheet generation using an LED. Ray colors denote individual light originated from different regions of the LED. CL, cylindrical lens; F1–2, lenses; IP, imaging plane; Obj, objective lens.

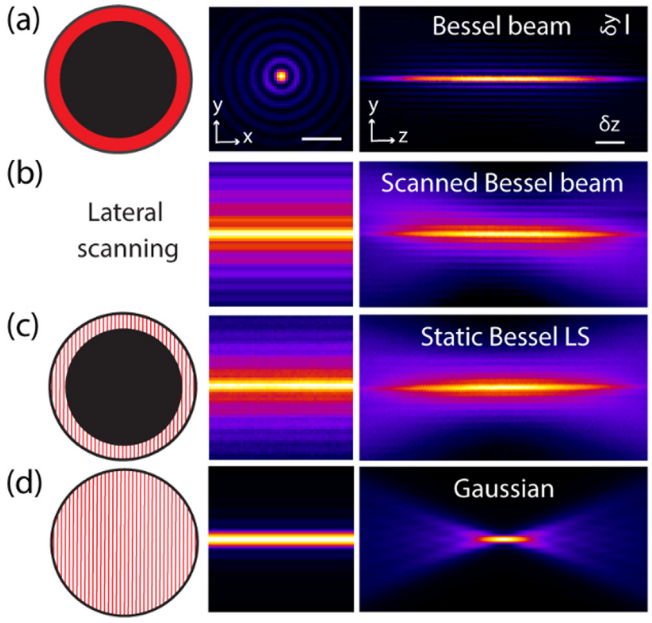

Fig. 3. Experimental results for a Bessel beam (a) and a scanned Bessel beam (b) generated with an annular ring and laser. Scale bars, δy = 40 μm and δz = 1 mm. (c, d) Static Bessel light-sheet (c) and Gaussian light-sheet (d) generated with 1D coherent beam from an LED.

Applied Image) placed at the BFP of the cylindrical lens to control the spatial coherence. Then the slit was conjugated to an image plane using a relay system composed of a lens F2 (f_2 = 50 mm, AC254-050-A) and an objective F3 (f_3 = 40 mm, AC254-040-A). An annular ring (R1CA2000) with outer (d_1) and inner (d_2) diameters of 2 mm and 1.75 mm, respectively, was inserted at the BFP of the objective. Lenses and optomechanics were purchased from Thorlabs unless specified otherwise. The beam emanating from the slit is a 1D coherent beam and instantaneously produces numerous focused lines at the different positions of the BFP while illuminating the entirety of the annular mask.

To measure the intensity profiles of the generated light-sheets, we placed a camera (DMK 33UX290; The Imaging Source) behind the objective and recorded images by moving the camera along the z-axis using a motorized stage driven by a servo motor (Thorlabs, PT1-Z8). For comparison, we first used a diode laser (λ = 638 nm, Cobolt) spatially filtered by a single mode fiber. In this case, a Bessel beam was generated as expected [Fig. 3(a)]. Its propagation length at the full width at half maximum (FWHM) was 6.90 mm, which was about 6 times longer than that of a Gaussian beam with a similar thickness [Fig. 3(d)]. In

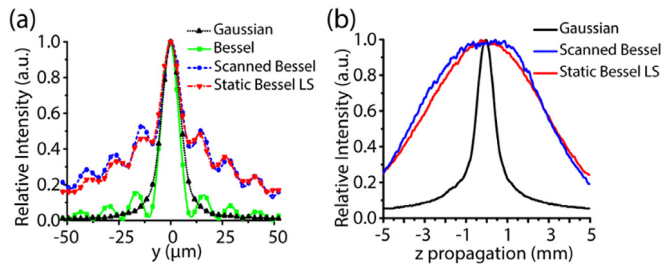

Fig. 4. Transverse (a) and propagation (b) profiles of Gaussian beam, Bessel beam, scanned Bessel beam and static Bessel light-sheet.

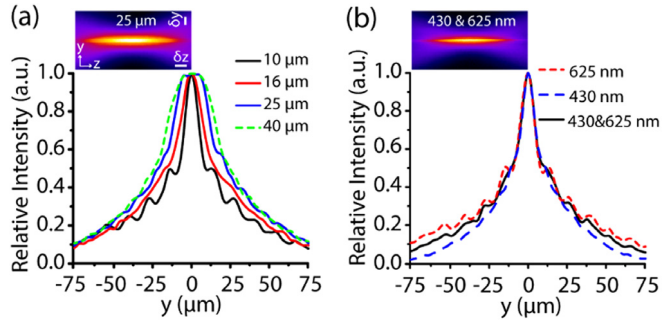

Fig. 5. (a) Intensity profiles along the y-axis for static Bessel light-sheets measured with different slit widths. (b) Dual color light-sheet generation at wavelengths of 430 nm and 625 nm. Scale bar, δy = 40 μm and δz = 1 mm.

contrast, with 1D coherent light from LED, a static non-diffracting light-sheet was generated without beam scanning [Fig. 3(c)]. Its propagation length was 6.75 mm and the beam thickness was ~14.5 μm [Fig. 4(a) and (b)], which were the same as those of a laterally scanned Bessel beam [Fig. 3(b)]. This was obtained by convolution of the measured Bessel beam intensity and a line along the x-axis. The lateral field-of-view along the x-axis of the static non-diffracting light-sheet was ~10 mm. Note that by increasing the ratio d_2/d_1 one can readily prepare a non-diffracting light-sheet with a longer propagation length; however, this results in substantial side-lobes that are not desirable for fluorescence imaging. If the annular ring mask is omitted, one can create static Gaussian light-sheets as well [Fig. 3(d)].

To examine the effect of the degree of spatial coherence, we measured the propagation intensity profiles with various slit widths. As the width increased from 10 μm to 40 μm, the beam thickness increased by 3.4-fold and the side-lobe fringes faded [19] while the propagation length remained almost constant [20][Fig. 5(a)]. The spatial coherence radius (ρ_c) at the BFP can be approximated as $\rho_c = \lambda f_2/D$ = 3.1 mm [18], which ensured high spatial coherence along the y-axis for our annular ring when used with the 10 μm slit.

Next, we examined the possibility of multicolor imaging. Two LEDs (λ = 430 nm and 625 nm) were combined by a dichroic beamsplitter and sent to the slit. The resulting light-sheets were approximately the same beam thickness [Fig. 5(b)], while the length of light-sheet at 430 nm was slightly shorter than that at 625 nm. The bandwidth of LED used (<20 nm) does not affect the properties of our light-sheets.

Lastly, instead of an LED, we used a diode laser (λ = 638 nm, Cobolt 06-MLD) but reduced its spatial coherence by coupling it into a multimode fiber (Ø400 μm, M28L01). A transmissive speckle reducer (Optotune, LSR-3005-12D-VIS) and a fiber shaker motor (ASLONG, JRF370-18260) were used to randomize speckle patterns and decrease the spatial coherence. For convenience, the beam was connected to a round-to-linear multimode fiber bundle (75 × Ø50 μm, custom design; Leoni) and the output beam was sent via a setup shown in Fig. 6(b). The same annular ring was used as in the LED experiment. This laser-based approach also generated a static non-diffracting light-sheet [Fig. 6(c)] with a negligible speckle pattern. We obtained ~0.5 mW of output power at the sample plane (0.36% efficiency), which was ~50 times higher illumination efficiency than an LED. However, it is possible to further improve the light efficiency by optimizing our setup. Approximately 60 fibers were mapped on the BFP and this was sufficient for a complete field synthesis [15].

4. Conclusions

We propose a new method to generate light-sheets by controlling the spatial coherence of light. A 1D coherent beam in conjunction with a spatial filter enables us to create non-diffracting light-sheets exhibiting uniform illumination and a long propagation length. Unlike other approaches, our method does not require lateral scanning and is also well suited to multicolor imaging. We can extend our approach to create other non-diffracting light-sheets as well [21,22]. Either an LED or a laser can be employed once their spatial coherence is properly controlled, yielding a 1D coherent beam. It is promising to use a laser with tunable spatial coherence [23] such as degenerate cavity lasers [24]. Our simple approach has potential for advancing LSFM systems [25], including generation of multiple light-sheets in 3D [26,27].

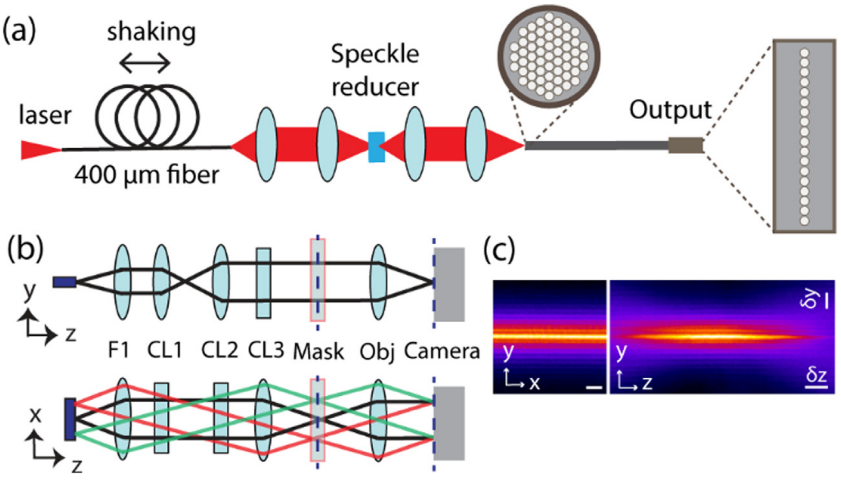

Fig. 6. (a, b) Schematic for preparing 1D coherent beam by a laser. (b) Experimental setup for single-shot nondiffracting light-sheet generation using a laser. F_1 = 50 mm, F_{CL1} = 10 mm, F_{CL2} = 50 mm, F_{CL3} = 25 mm, F_{obj} = 40 mm. (c) The generated static Bessel light-sheet. The exposure time of camera was 20 ms. Scale bar, δy = 40 μm and δz = 1 mm.

Declaration of competing interest

The authors declare the following financial interests/personal relationships which may be considered as potential competing interests: University of Central Florida has filed a patent application covering the work described in this paper.

Acknowledgments

We thank Ayman Abouraddy for fruitful discussion and Benjamin Croop for critically reading our manuscript.

Funding

National Institutes of Health, USA (R21GM131163) and National Science Foundation, USA (1805200).

References

[1] H. Siedentopf, R. Zsigmondy, Ann. Phys. 315 (1902) 1–39.
[2] T. Mappes, N. Jahr, A. Csaki, N. Vogler, J. Popp, W. Fritzsche, Angew. Chem. Int. Ed. 51 (2012) 11208–11212.
[3] J. Huisken, J. Swoger, F. Del Bene, J. Wittbrodt, E.H.K. Stelzer, Science 305 (2004) 1007–1009.
[4] P.J. Keller, M.B. Ahrens, Neuron 85 (2015) 462–483.
[5] O.E. Olarte, J. Andilla, E.J. Gualda, P. Loza-Alvarez, Adv. Opt. Photon. 10 (2018) 111–179.
[6] J.M. Girkin, M.T. Carvalho, J. Opt. 20 (2018) 053002.
[7] A.-K. Gustavsson, P.N. Petrov, W.E. Moerner, Opt. Express 26 (2018) 13122–13147.
[8] P.J. Keller, A.D. Schmidt, J. Wittbrodt, E.H.K. Stelzer, Science 322 (2008) 1065–1069.
[9] F.O. Fahrbach, P. Simon, A. Rohrbach, Nature Photon. 4 (2010) 780–785.
[10] T.A. Planchon, L. Gao, D.E. Milkie, M.W. Davidson, J.A. Galbraith, C.G. Galbraith, E. Betzig, Nature Methods 8 (2011) 417–423.
[11] T. Vettenburg, H.I.C. Dalgarno, J. Nylk, C. Coll-Llado, D.E.K. Ferrier, T. Cizmar, F.J. Gunn-Moore, K. Dholakia, Nature Methods 11 (2014) 541–544.
[12] F.O. Fahrbach, V. Gurchenkov, K. Alessandri, P. Nassoy, A. Rohrbach, Opt. Express 21 (2013) 11425–11440.
[13] R.M. Power, J. Huisken, Nature Methods 14 (2017) 360–373.
[14] J. Tang, J. Ren, K.Y. Han, Nanophotonics 8 (2019) 2111–2128.
[15] B.-J. Chang, M. Kittisopikul, K.M. Dean, P. Roudot, E.S. Welf, R. Fiolka, Nature Methods 16 (2019) 235–238.
[16] H.E. Kondakci, A.F. Abouraddy, Nature Photon. 11 (2017) 733–740.
[17] M. Yessenov, B. Bhaduri, H.E. Kondakci, M. Meem, R. Menon, A.F. Abouraddy, Optica 6 (2019) 598–607.
[18] B.E.A. Saleh, M.C. Teich, Fundamentals of Photonics, third ed., Wiley, New York, 2019.
[19] P. Fischer, C.T.A. Brown, J.E. Morris, C. López-Mariscal, E.M. Wright, W. Sibbett, K. Dholakia, Opt. Express 13 (2005) 6657–6666.
[20] J. Turunen, A. Vasara, A.T. Friberg, J. Opt. Soc. Amer. A 8 (1991) 282–289.
[21] B.-C. Chen, W.R. Legant, K. Wang, L. Shao, D.E. Milkie, M.W. Davidson, C. Janetopoulos, X.S. Wu, J.A. Hammer, III, Z. Liu, B.P. English, Y. Mimori-Kiyosue, D.P. Romero, A.T. Ritter, J. Lippincott-Schwartz, L. Fritz-Laylin, R.D. Mullins, D.M. Mitchell, J.N. Bembenek, A.-C. Reymann, R. Boehme, S.W. Grill, J.T. Wang, G. Seydoux, U.S. Tulu, D.P. Kiehart, E. Betzig, Science 346 (2014) 439.
[22] B.-J. Chang, R. Fiolka, J. Phys. Photon. 2 (2020) 014001.
[23] H. Cao, R. Chriki, S. Bittner, A.A. Friesem, N. Davidson, Nat. Rev. Phys. 1 (2019) 156–168.
[24] R. Chriki, M. Nixon, V. Pal, C. Tradonsky, G. Barach, A.A. Friesem, N. Davidson, Opt. Express 23 (2015) 12989–12997.
[25] R.M. Power, J. Huisken, Nature Methods 16 (2019) 1069–1073.
[26] G. Calisesi, M. Castriotta, A. Candeo, A. Pistocchi, C. D'Andrea, G. Valentini, A. Farina, A. Bassi, Biomed. Opt. Express 10 (2019) 5776–5788.
[27] Y.-X. Ren, J. Wu, Q.T.K. Lai, H.M. Lai, D.M.D. Siu, W. Wu, K.K.Y. Wong, K.K. Tsia, Light Sci. Appl. 9 (2020) 8.